Operational correction for the temperature dependence of a class of hyperspectral radiometers

Giuseppe Zibordi[1,2] and Marco Talone[3]

[1]*National Aeronautics and Space Administration, Goddard Space Flight Center, Greenbelt, MD, USA*

[2]*Southeastern Universities Research Association, Washington, DC 20005, USA*

[3]*Departament de Oceanografía Física i Tecnològica, Institut de Ciències del Mar (ICM-CSIC) and the Barcelona Expert Centre (BEC), 08003 Barcelona, Spain*

Corresponding author: Giuseppe Zibordi, giuseppe.zibordi@eoscience.eu

ABSTRACT

The correction for temperature response of optical radiometers implies access to their working temperature (*i.e.*, either the internal or ambient one, with the radiometers in thermal equilibrium). With specific reference to a class of widely used hyperspectral radiometers lacking a thermistor to measure the internal temperature, this work investigated the potential for operational corrections relying on the working temperature derived from the radiometer dark signal. With the objective to keep within approximately 1% the uncertainty for corrections in the 400-800 nm spectral range, findings show the applicability of the method for working temperatures higher than approximately 30°C. The complementary use of the air temperature, regardless of an expected error of several degrees with respect to the actual radiometer working one, appears a valid solution for temperatures lower than 30°C.

1. Introduction

Satellite data products satisfy application needs and ensure return on investment when they meet users requirements. Therefore, the verification of these requirements is a mandatory step for satellite data products, which are often generated through complex processes involving remote technology, indirect sensor calibration, and a number of algorithms and models. This verification commonly requires access to *in situ* reference data of high accuracy entailing: state-of-the-art absolute radiometric calibration and comprehensive characterization of field radiometers; accurate implementation of measurement protocols; and finally, reduction of collected data applying severe quality control procedures.

Temperature affects the performance of the optical, electrical and mechanical components of radiometers (Basher and Matthews 1977, Starks et al 1995, Hartmann et al. 2001, Kuusk 2011, Pacheco-Labrador and Martín 2015). For instance, the temperature response of silicon photodiodes varies across the spectrum. It is quite moderate in the blue and green spectral regions, but significantly increases with wavelength (McCluney 2016). Because of this, in the absence of a thermal stabilization, the response to temperature of individual radiometers or alternatively of sample units representing classes of radiometers, is essential (Schaepman and Dangel 2000, Salim et al 2011, Zibordi et al 2017).

With the objective to minimize errors in *in situ* radiometric measurements and best support the quantification of uncertainties affecting satellite data products, a specific investigation targeted the determination of the coefficients describing the change in response with temperature of a class of hyperspectral RAMSES radiometers (TriOS Mess-und Datentechnik GmbH; Rastede, Germany) widely applied by the ocean color community. Due to the lack of a thermal stabilization and also of a thermistor allowing to measure the internal temperature, their temperature response was determined with respect to the ambient one assuming the instrument was in thermal equilibrium with it. Characterizations performed in the 400-800 nm spectral range with radiometer working temperatures in the 10-40 °C interval, showed mean temperature coefficients varying from -0.04×10^{-2} $(°C)^{-1}$ at 400 nm to $+0.33\times10^{-2}$ $(°C)^{-1}$ at 800 nm. The former findings, when assumed applicable to the specific class of hyperspectral radiometers, indicated the possibility to determine temperature corrections with an uncertainty of approximately 0.03×10^{-2} $(°C)^{-1}$.

This work primarily investigates the potential for determining the working temperature from the dark signal of the considered class of hyperspectral radiometers.

2. The radiometers

RAMSES hyperspectral radiometers are built on ZEISS (Oberkochen, Germany) Monolithic Miniature Spectrometers (MMS-1) with the Hamamatsu (Ichino-cho, Japan) S3904 256-channel silicon photodiode array coupled to a concave image grating (Hamamatsu 2006, Hamamatsu 2016). The optics of RAMSES ARC radiance sensors, exhibiting a 7 degrees full angle field-of-view, is composed of an optical window and a lens coupled to the fiber-bundle supplying light to the spectrometer. Conversely, the RAMSES ACC irradiance sensors have a cosine collector coupled to the fiber-bundle. A steel case encloses optics, spectrometer and electronics. RAMSES radiometers have a spectral resolution of approximately 10 nm in the 320-950 nm interval with an average spectral sampling of 3.3 nm.

3. Dark signal dependence on temperature

The working temperature of radiometers largely affects their dark signal (*i.e.,* the radiometer output in the absence of any input flux), as well as their response. When sensors do not allow for an automatic determination of the dark signal (*e.g.*, in the absence of an internal shutter), dedicated measurements should be performed by occluding the sensor optics. An inappropriate quantification of the dark signal would lead to poor bias corrections of radiometric quantities with unavoidable impact on the final radiometric data products. Additionally, corrections for temperature response should be applied to any radiometric measurement accounting for dedicated characterizations. As already anticipated, this step requires access to the internal or alternatively to their external working temperature, depending how characterizations were performed.

The dark signal of RAMSES radiometers is operationally obtained from the output of a group of detector elements painted black (*i.e.,* the array elements from 237 to 254). Alternatively, it can be determined for each element of the detector array by performing measurements with the optics occluded.

Laboratory investigations of the dark signal for RAMSES radiometers confirmed a clear dependence with temperature and naturally with the integration time (see Fig. 1a). Consequently, when considering the possibility to quantify the radiometer working temperature from the dark signal, the most accurate information could be obtained with long integration times. Figure 1b illustrates such a dependence of the dark signal determined with diverse integration times. Remarkably, the temperature dependence on dark digital counts in

Fig. 1a, well documents a low sensitivity below tentatively 30 °C. This anticipates low accuracy for any radiometer working temperature quantified using the dark signal at relatively low temperatures.

Figure 1b also shows that the charge overflow (*i.e.*, the transfer of charge from saturated elements of the array to the nearby ones) prevents determining the dark signal from the dark-painted elements simply applying a high integration time without occluding the optics. In fact, the black-painted cells would be perturbed by charge overflow from the nearby elements affected by saturation due to over exposition to a light source.

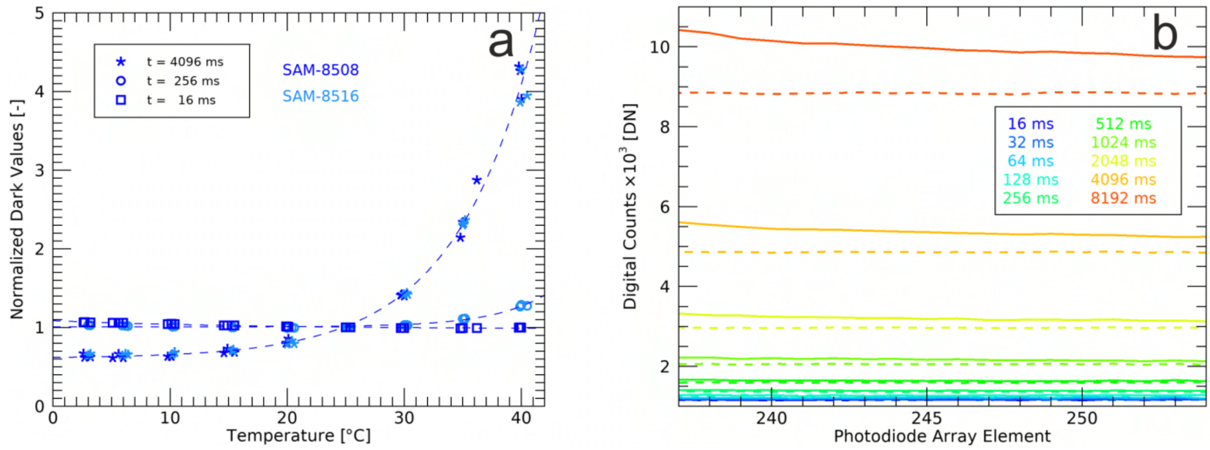

Fig. 1. (a) Dark digital counts normalized at $T = 25$ °C determined for RAMSES SAM-8508 and RAMSES SAM-8516 with different integration times *t*, and (b) dark digital counts *DN* determined from the black-painted elements of SAM-8516 with the entrance optics occluded (dashed lined) and alternatively illuminated by an integrating sphere with saturation occurring for $t > 256$ ms (continuous line) (after Zibordi et al. 2017).

4. Relationship between dark signal and temperature

Dark digital counts *DN* for various RAMSES radiometers at diverse ambient temperatures *T* were obtained from laboratory measurements performed in a thermal tank with the entrance optics occluded and relying on the factory default integration time (*i.e.,* 4096 ms for dark signal measurements). Results for SAM-8516 are summarized in Fig. 2 through the fit of the working **t**emperatures *T* as a function of *DN*

$$T = -T_C + S * \ln(DN - DN_C) \quad (1)$$

where the digital dark value DN_C, the temperature T_C and the slope factor S are obtained from the fit.

The smallest changes in derived working temperatures from dark digital counts (*i.e.*, the sensitivity) are displayed in Fig. 2b. These values further confirm the limits in determining accurate working temperatures from dark digital counts lower than approximately 3×10^3, which correspond to temperatures lower than approximately 30°C.

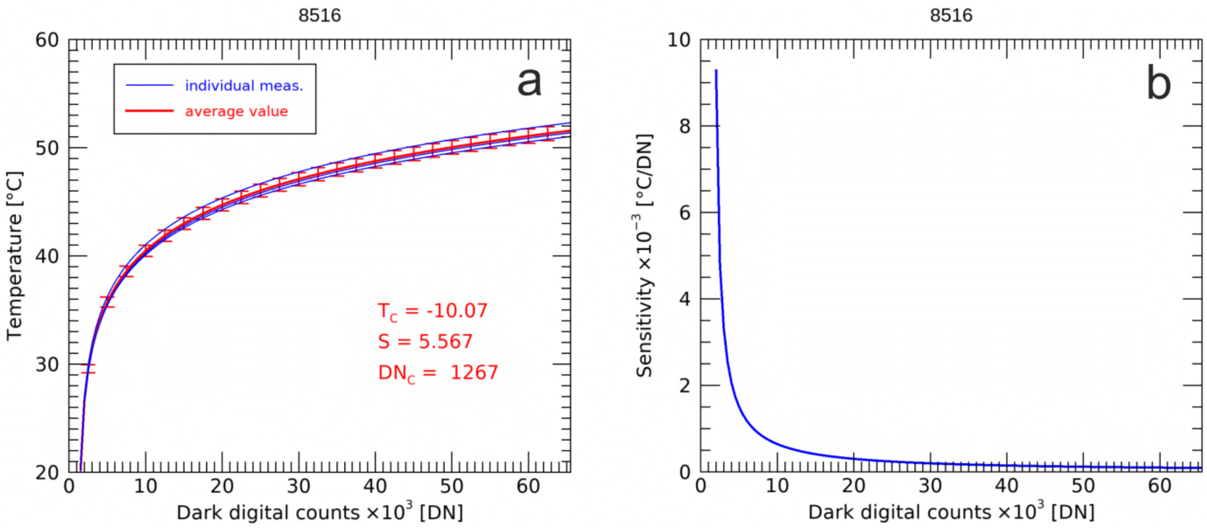

Fig. 2. (a) Working temperature *T* and (b) temperature sensitivity vs. dark digital counts *DN* as obtained for SAM-8516 from three independent characterizations performed with integration time *t* = 4096 ms by occluding the entrance optics. The fitted values in (a) result from the application of Eq. 1 with T_C = 10.07, S = 5.567 and DN_C=1267, while the error bars indicate ±1 standard deviation.

5. Temperature determination

The need to apply corrections for the temperature response of RAMSES radiometers, which is necessary to meet uncertainty requirements for remote sensing applications (IOCCG 2019), suggests to investigate operational solutions allowing to determine the radiometer working temperature from the dark signal. Figure 3 summarizes such an attempt through the average of the fits performed applying Eq. 1 the characterization data from four RAMSES radiometers: three irradiance sensors (serial numbers SAM-835C, SAM-82C1, and SAM-8516) and one RAMSES radiance sensor (serial number SAM-8508). The standard deviation $\sigma_T(DN)$ of the averaged values, which largely increases with a decrease of the dark digital counts, determines the uncertainties of the fitting function. In particular, whereas an uncertainty in the working temperature *T* expressed by $\sigma_T(DN)$ is approximately 2°C with 1×10^4 digital counts, its value approaches 5°C with 3×10^3 digital counts.

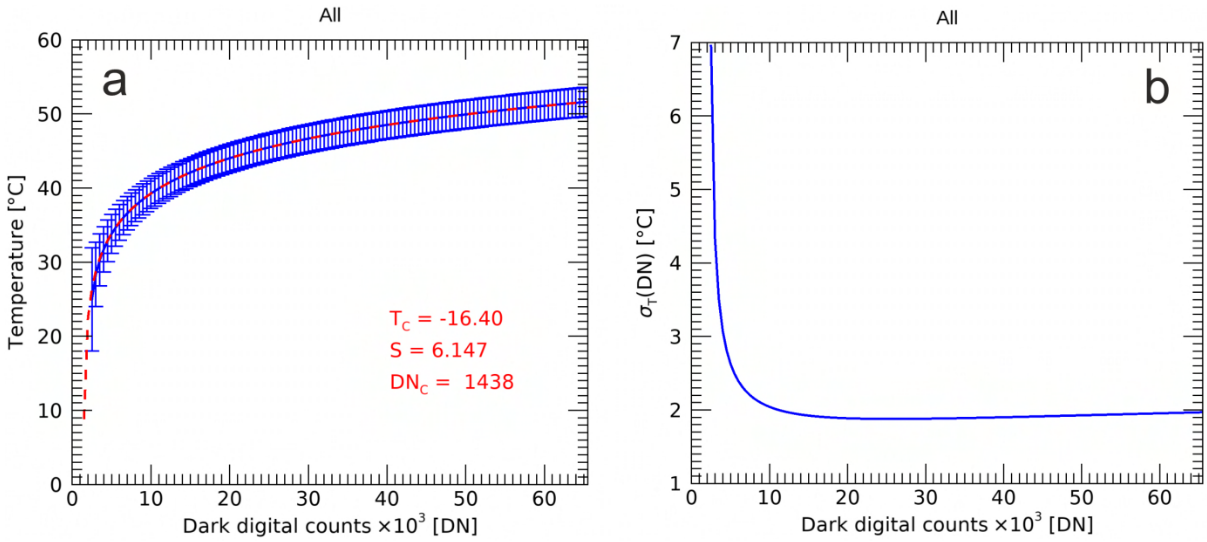

Fig. 3. (a) Working temperature T and (b) related standard deviation $\sigma_T(DN)$ as a function of the dark digital counts DN determined from the characterization of SAM-82C1, SAM-835C, SAM-8508 and SAM-8516. The error bars in (a) indicate $\pm 1\ \sigma_T(DN)$.

Mean temperature coefficients $c(\lambda)$ as a function of wavelength λ with uncertainty defined by $\sigma_c(\lambda)=0.03\times10^{-2}$ $(°C)^{-1}$ in the 400-800 nm spectral range for the 10-40°C interval for ambient temperature, were provided by Zibordi et al (2017) for the class of RAMSES radiometers. These coefficients are denoted as

$$c(\lambda) = k_0\left\{1 - \sum_{i=1}^{4}[k_i(\lambda-400)]^i\right\} \quad (2)$$

with $k_{0\text{-}4}$ = [-0.000347, +0.011266, +0.010078, -0.007950, +0.005386].

Following Zibordi et al (2017), the relative spectral change $R_r(\lambda, \Delta T)$ affecting radiometric values due to the difference ΔT between the working temperature T during field operations and the laboratory one T_0 recorded during the radiometer absolute calibration (*i.e.*, $\Delta T = T\text{-}T_0$), is given by

$$R_r(\lambda, \Delta T) = c(\lambda) \times \Delta T. \quad (3)$$

By introducing $\varepsilon_c(\lambda, \Delta T)$ and $\varepsilon_T(\lambda, DN)$, which determine the non-correlated relative uncertainties affecting $c(\lambda)$ and ΔT, respectively, with

$$\varepsilon_c(\lambda, \Delta T) = \Delta T \times \sigma_c(\lambda) \quad (4)$$

and

$$\varepsilon_T(\lambda, DN) = c(\lambda) \times \sigma_T(DN)\,, \tag{5}$$

the combined uncertainty affecting $R_r(\lambda, \Delta T)$ is then given by

$$u_r(\lambda, \Delta T, DN) = [\varepsilon_c(\lambda, \Delta T)^2 + \varepsilon_T(\lambda, DN)^2]^{1/2}. \tag{6}$$

Figure 4 displays the values of $R_r(\lambda, \Delta T)$ obtained for the 0-50°C interval omitting any uncertainty contribution. These values are well within ±1% in the 400-500 nm spectral interval regardless of the working temperature (it is recalled that the working temperature is here the ambient one with the radiometer in thermal equilibrium). Nevertheless, the values of $R_r(\lambda, \Delta T)$ at 700 nm reach +5% with T = 50°C and -4% with T = 0°C.

Assuming both $\sigma_c(\lambda)$ and $\sigma_T(DN)$ are representative for the class of RAMSES radiometers, Fig. 5a shows the separate contributions of $\varepsilon_c(\lambda, \Delta T)$ and $\varepsilon_T(\lambda, DN)$ to the uncertainties affecting $R_r(\lambda, \Delta T)$ with T in the 0-50°C interval. While $\varepsilon_c(\lambda, \Delta T)$ is always within ±1% regardless of the value of T, $\varepsilon_T(\lambda, DN)$ exceeds 1% beyond 550 nm for T tentatively lower than 30°C in agreement with the large values of $\sigma_T(DN)$ (see Fig. 3b). Consistently, the combined uncertainties $u_r(\lambda, \Delta T, DN)$ displayed in Fig. 5b show values generally lower than 1% up to 550 nm regardless of T, but already approaching 2% at 700 nm for T = 20°C and further increasing for lower temperatures.

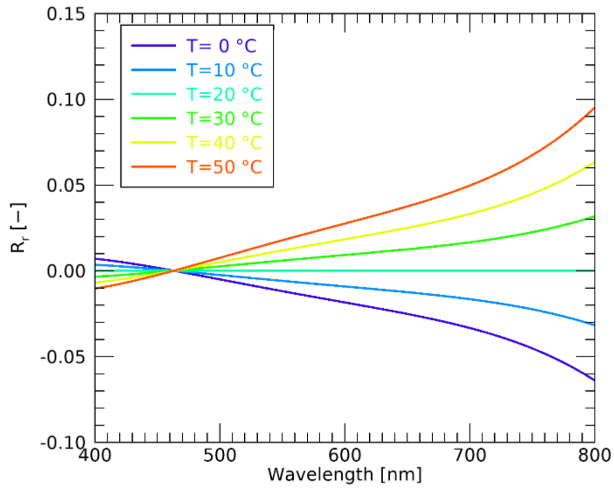

Fig. 4. Class based values of $R_r(\lambda, \Delta T)$ determined assuming null both $\sigma_c(\lambda)$ and $\sigma_T(DN)$.

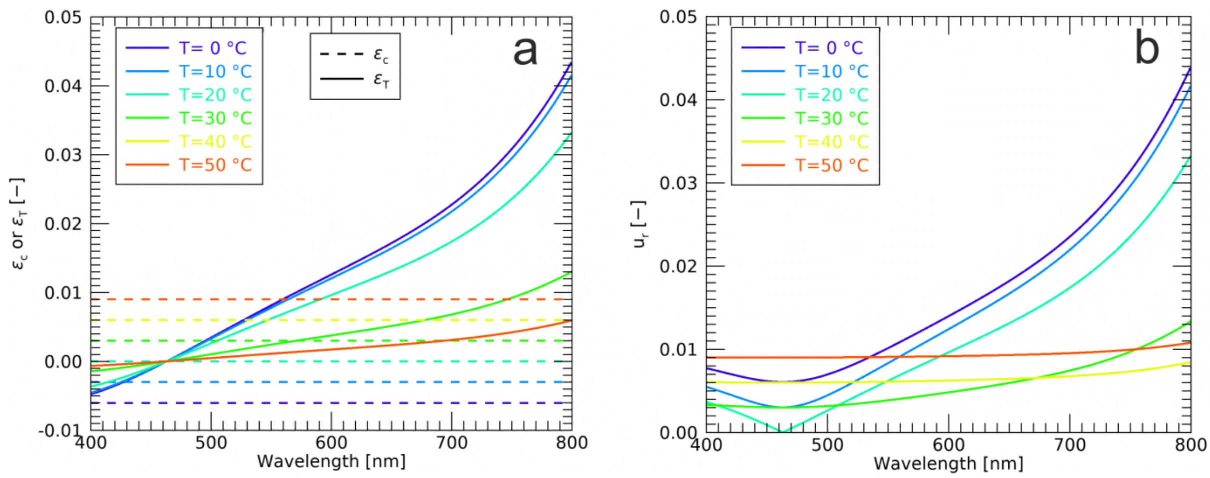

Fig. 5. (a) Spectral values of $\varepsilon_c(\lambda, \Delta T)$ and $\varepsilon_T(\lambda, DN)$ and (b) corresponding $u_r(\lambda, \Delta T, DN)$. Computations were made for $T_0 = 20$°C and T in the range of 0-50°C.

6. Discussion

Findings in Section 5 indicate that when targeting uncertainties lower than 1% for the correction of RAMSES temperature response across the 400-800 nm spectral range, the determination of the radiometer working temperature T from the dark signal obtained with integration time $t = 4096$ ms and entrance optics occluded, is only viable for $T > 30$°C. This calls for alternative solutions allowing to estimate the radiometer working temperature during field operations.

Definitively, accurate ambient temperatures T representative of the radiometer working one diverge from the air temperature T_a. In fact, the direct sun light affects the actual radiometer working temperature with impact varying with the instrument location and orientation. An estimate of the difference between air and RAMSES working temperatures was obtained by measuring the temperature in the proximity of the radiometer case inside a 1 cm thick steel sleeve enfolding the radiometer itself. This approach showed differences between the ambient temperature measured inside the sleeve and the actual air one in the course of daily operations, ranging from negligible values up to approximately 5°C when the radiometer was exposed to the direct sun light during clear sky and air temperatures of 27°C. Fully admitting that these differences are only indicative for actual field measurement, still to estimate the impact of applying corrections exclusively relying on the knowledge of T_a (*i.e.*, assuming $T \sim T_a$), constant biases $\delta T = +5$°C and $\delta T = +10$°C are hereafter considered as tentative maximum differences between T and T_a (*i.e.*, $T = T_a + \delta T$).

By defining

$$\varepsilon_T^*(\lambda, \delta T) = c(\lambda) \times \delta T \tag{9}$$

the contribution to the uncertainty affecting $c(\lambda)$ and solely due to δT, the relative uncertainty $u_r^*(\lambda, \Delta T, \delta T)$ for $R_r(\lambda, \Delta T)$ is then given by

$$u_r^*(\lambda, \Delta T, \delta T) = [\varepsilon_c(\lambda, \Delta T)^2 + \varepsilon_T^*(\lambda, \delta T)^2]^{1/2}. \tag{10}$$

Figure 6a shows the impact of $\varepsilon_c(\lambda,\Delta T)$ and $\varepsilon_T^*(\lambda,\delta T)$ on $R_r(\lambda,\Delta T)$. Their combined contributions lead to uncertainties $u_r^*(\lambda,\Delta T,\delta T)$ lower than approximately 1% up to 700 nm when quantified with $\delta T = +5$°C for $T_0 = 20$°C regardless of T in the range of 0-40°C. For the same conditions, $u_r^*(\lambda,\Delta T,\delta T)$ slightly exceeds 1% for the extreme working temperature T = 50°C. When considering δT = +10°C the values of $u_r^*(\lambda,\Delta T,\delta T)$ already exceed 1% beyond 500 nm and approach 2% at 700 nm. This finding shows that when allowing uncertainties up to approximately 1% for the correction of temperature response, the assumption of equivalence between radiometer working temperature and that of the air is a valid solution for differences $\delta T = T\text{-}T_a$ not exceeding +5°C. Indeed, the combined use of both the working temperature determined from the dark signal for $T > 30$°C and alternatively assuming $T = T_a$ for $T < 30$°C provides an adequate solution for operational field applications across the 400-800 nm spectral interval.

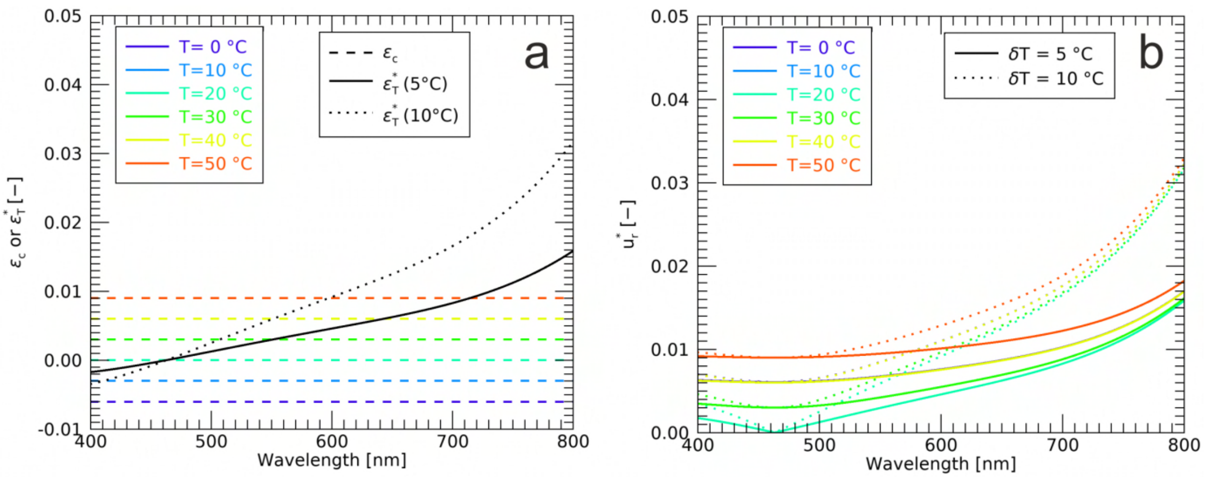

Fig. 6. (a) Values of $\varepsilon_c(\lambda,\Delta T)$ and $\varepsilon_T^*(\lambda,\delta T)$ and (b) corresponding $u_r^*(\lambda, \Delta T, \delta T)$. Computations were made for T_0 = 20°C assuming the radiometer working temperature determined with biases δT = +5°C and δT = +10°C and T within the range 0-50°C.

7. Summary and conclusions

Considering the lack of an internal thermistor, this study primarily investigated the potential for determining the instrument working temperature from the dark signal of RAMSES radiometers. The analysis was performed applying corrections assumed applicable to the class of instruments and determined with *i*. temperature coefficients and *ii*. relationships between dark signal and working temperatures. Results, based on dark digital counts obtained occluding the entrance optics of the radiometers and applying an integration time t = 4096 ms, indicate the possibility to perform temperature corrections with uncertainties lower than 1% in the 400-800 nm interval for working temperatures T higher than approximately 30°C. Uncertainties may exceed 3% at 800 nm for T lower than approximately 30°C due to the lesser sensitivity of temperature retrievals with the decrease of dark digital counts.

Still recognizing that the working temperature T would exhibit differences with the air temperature T_a, the study shows that the basic assumption of $T \sim T_a$ with $T\text{-}T_a < +5\%$ for $T < 30°C$, would allow to determine corrections with uncertainty within 1% up to 700 nm. This finding suggests that the complementary use of air temperature and temperature determined from the dark signal of RAMSES radiometers, would allow correcting temperature response with uncertainty constrained within 1% in the 0-50°C interval across the 400-800 nm spectral range.

Acknowledgements

G. Zibordi was supported by National Aeronautics and Space Administration through the Southeastern Universities Research Association, Goddard Earth Sciences Technology and Research II Award, grant 80NSSC22M0001. M. Talone was supported by the “Severo Ochoa Centre of Excellence” Accreditation under Grant CEX2019-000928-S

Data availability statement

The laboratory data applied in the study are available from the authors.

REFERENCES

Basher, R. E., and W. A. Matthews, 1977: Problems in the use of interference filters for spectrophotometric determination of total ozone. *J. Appl. Meteorol*. **16**, 795–802.

Hamamatsu, 2006: *Si photodiode S2386 series*. HAAMMATSU PHOTONICS K.K., Solid State Division, Ichino-cho, pp. 4. Accessible at http://shpat.com/docs/hamamatsu/S2386_series.pdf.

Hamamatsu, 2016: *Characteristics and use of NMOS linear image sensors*. *Technical Information SD-26*. HAAMMATSU PHOTONICS K.K., Solid State Division, Ichino-cho, pp. 49. Accessible at https://www.hamamatsu.com/resources/pdf/ssd/nmos_kmpd9001e.pdf .

Hartmann, J., J. Fischer, U. Johannsen, and L. Werner, 2001: Analytical model for the temperature dependence of the spectral responsivity of silicon. *JOSA B*, **18**, 942–8947.

IOCCG (2019). Protocols for Satellite Ocean Colour Data Validation: In Situ Optical Radiometry. Zibordi, G., Voss, K. J., Johnson, B. C. and Mueller, J. L. IOCCG Ocean Optics and Biogeochemistry Protocols for Satellite Ocean Colour Sensor Validation, Volume 3.0, IOCCG, Dartmouth, NS, Canada. http://dx.doi.org/10.25607/OBP-691.

Kuusk, J., 2011: Dark signal temperature dependence correction method for miniature spectrometer modules. *J. Sens.*, doi:10.1155/2011/608157.

McCluney, W.R., 2014: *Introduction to radiometry and photometry*. Boston, Artech House, pp. 461.

Schaepman, M. E., and S. Dangel, 2000: Solid laboratory calibration of a nonimaging spectroradiometer, *Appl. Opt*. **39**, 3754–3764.

Pacheco-Labrador, J., and M. P Martín, 2015: Characterization of a field spectroradiometer for unattended vegetation monitoring. Key sensor models and impacts on reflectance. *Sensors* **15**(2), 4154-4175.

Salim, S.G., N.P. Fox, E. Theocharous, T. Sun, and K.T. Grattan, 2011: Temperature and nonlinearity corrections for a photodiode array spectrometer used in the field. *Appl. Opt.,* **50**, 866–875.

Starks, P.J., E. A. Walter-Shea, F. R. Schiebe and B. L. Markham, 1995: Temperature sensitivity characterization of a silicon diode array spectrometer. *Remote Sens. Environ.*, 51, 385–389.

Zibordi, G., Talone, M., and Jankowski, L., 2017: Response to temperature of a class of in situ hyperspectral radiometers. *J. Atmos. Ocean. Technol.,* 34(8), 1795–1805.